JOURNAL OF APPLIED ELECTROCHEMISTRY 21 (1991) 261–266

Influence of some organic compounds on the corrosion mechanism of carbon steel (XC38) in 3% NaCl II. Orthoaminothiophenol (C_6H_7NS) and surfactant dodecyl sodium phosphate ($C_{10}H_{21}PO_4Na_2$)

A. BEN-BACHIR, A. SRHIRI*

Université Mohamed V, Faculty of Sciences, Kenitra, Marocco

F. DABOSI

Equipe de Recherche Associée au CNRS no. 263, Laboratoire de Métallurgie Physique, Ecole nationale Supérieure de Chimie, 31077 Toulouse Cédex, France

Y. DERBALI

Department of Chemistry, Faculty of Sciences, Tunis, Tunisia

M. ETMAN

Laboratoire d'Electrochimie Interfaciale du CNRS, 1 Place A. Briand, 92195 Meudon Cédex, France

A. LATTES

Laboratoire IMRCP, Université Paul Sabatier, 31062 Toulouse, France

Received 12 December 1989; revised 22 May 1990

This paper presents an investigation of the influence of added organic compounds on the electrochemical behaviour of the carbon steel (XC38) in stirred and aerated 3% NaCl. Steady-state and transient measurements have been made using a rotating disc electrode. The influence of dodecyl sodium phosphate ($C_{10}H_{21}PO_4Na_2$) and orthoaminothiophenol (C_6H_7NS) have been studied. Results obtained allowed corrosion inhibition mechanism to be established. The nature of the electrode process has been elucidated.

1. Introduction

Many studies have already been made on the corrosion and inhibition of steels in acid media. These have included measurements on the corrosion rate and the identification of the elementary processes involved. However, studies in neutral media are relatively few [1–4]. One reason is probably the formation, in this case, of insoluble corrosion products which adhere to the surface of the working electrode [5–8]. In this paper the effect of the surfactant dodecyl sodium phosphate on the corrosion mechanisms of carbon steel (XC38) has been studied. For comparison, the influence of a non-surfactant, orthoaminothiophenol, has also been investigated. This study is an extension of previous work on the influence of surfactant compounds on the corrosion of carbon steel (XC38) in 3% NaCl [9].

2. Experimental details

The various experimental procedures and conditions are the same as those adopted in our previous paper [9].

3. Experimental results

3.1. *Carbon steel (XC38) – 3% NaCl + 5 × 10^{-2} M $C_{10}H_{21}PO_4Na_2$*

The effect of the addition of 5 × 10^{-2} M dodecyl sodium phosphate on the response to potentiostatic cathodic polarization of the rotating carbon steel (XC38)–3% NaCl interface is shown in Fig. 1. A diminution of cathodic current densities accompanied by a shift of E_{corr} towards positive values is noticed (unless otherwise mentioned, i and I refer to current density and applied or measured current, respectively). When the potential range is restricted, a limiting diffusion plateau current appears at higher negative potential values. The plateau current is much less than that obtained with the blank (Fig. 1a). The significant potential difference between E_{corr} and the potential at which the diffusion plateau starts corresponds to a

* To whom all correspondence should be addressed.

0021-891X/91 $03.00 + .12

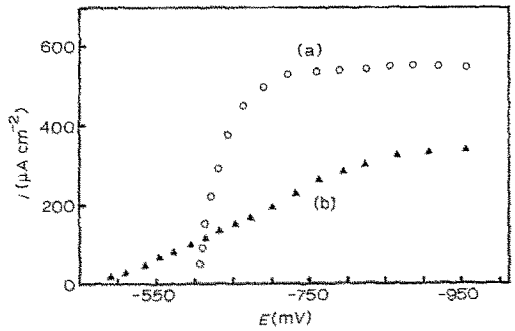

Fig. 1. Current–voltage characteristics with cathodic potentiostatic polarization; electrode maintained at E_{corr} for 30 min before measurements, electrode revolution per unit time, $N = 830$ r.p.m. (a) Carbon steel (XC38) – 3% NaCl, (b) carbon steel (XC38) – 3% NaCl + 5×10^{-2} M $C_{10}H_{21}PO_4Na_2$.

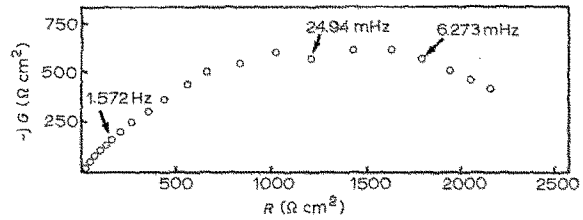

Fig. 2. Electrochemical galvanostatic impedance diagram in the presence of 5×10^{-2} M $C_{10}H_{21}PO_4Na_2$, $i = 0\,\mu A\,cm^{-2}$; electrode maintained at E_{corr} for 45 min before measurements and $N = 1000$ r.p.m. G is the imaginary component of the impedance in the complex plane ($Z = R - jG$) where $j = (-1)^{1/2}$.

mixed kinetic potential range. This is confirmed by a cathodic Tafel straight line after diffusion corrections have been made. From the extrapolation of the Tafel line to E_{corr}, $i_{corr} = 40\,\mu A\,cm^{-2}$. The efficiency of corrosion inhibition was estimated to be 94%.

When the working electrode is maintained for 45 min at its corrosion potential, E_{corr}, the galvanostatic impedance diagrams in Fig. 2 are obtained. Only one open capacity loop with a very low characteristic frequency (F_c), 25 mHz, is noticed. From the extrapolation of this loop to zero frequency, the global resistance ($R_p + R_E$) is estimated to be $2600\,\Omega cm^2$. This is the sum of polarization resistance and the electrolyte resistance and is in good agreement with the value obtained from the current–potential curves: $(dE/di)_{i \to 0}$. The associated capacity of this loop is $\sim 2.5\,mF\,cm^{-2}$, a high value with respect to the value generally attributed to the capacity of the double layer ($20–100\,\mu F\,cm^{-2}$). With the electrode surface free from corrosion products and taking into consideration arguments presented earlier [10], this high capacity value of $2.5\,mF\,cm^{-2}$ cannot be attributed to an increase of the specific area due to the development of a film of corrosion products. When the high frequency range of Fig. 2 is considered, a linear relationship between log G and log F is observed (see Fig. 3). Such a result is characteristic of Warburg impedance indicating a relaxation of concentration. This loop can be attributed to strongly linked mass transport and charge transfer processes. This hypothesis is consistent with the low value of $i_{corr} \simeq 40\,\mu A\,cm^{-2}$, calculated from the relation of Stern and Geary [11].

Increasing the time the working electrode is held for pretreatment in the electrolyte before taking measurements; this results in the appearance on the impedance diagrams of a loop at high frequencies (see Fig. 4). The parameters associated with this high frequency loop are assembled in Table 1. The attribution of this loop to charge transfer is in conflict with the corrosion inhibition efficiency calculated above for the following reasons: (i) R_{HF} ($14\,\Omega cm^2$) < R_{blank} ($100\,\Omega cm^2$) leading to a significant increase of corrosion rate despite the fact that a high inhibition efficiency of $\simeq 94\%$ is observed; (ii) for charge transfer, R_T must decrease regularly with increasing overvoltage which is not the case here (see Table 1).

The high frequency loop discovered by other investigators has already been attributed to the establishment of a relatively thick and compact film [12–14]. If we accept this interpretation for the present study, this means that the corrosion products would participate in the growth of the film. In fact, the high frequency loop appears when the electrode is immersed in the electrolyte for a long time at E_{corr} before measurements are effected and in the anodic domain only. In addition to the high frequency loop, a low frequency loop is observed, this representing a faradaic process taking place on the free electrode sites. The capacity value of the low frequency loop (C_{BF}), its characteristic frequency value ($F_{C_{BF}}$) and of its associated resistance (R_{BF}) are reported in Table 1. On increasing the anodic overvoltage, a significant drop of C_{BF} is observed. Compared with C_{BF} at $i = 0\,\mu A\,cm^{-2}$, the lowest value of C_{BF} is at $i_a = 50\,\mu A\,cm^{-2}$. This probably corresponds to a reduction of the active surface of the electrode due to the establishment of a porous film.

For $i_a = 120$ and $200\,\mu A\,cm^{-2}$, the capacity of the low frequency loop drops abruptly to low values, lower than those obtained generally for the double layer capacity ($\sim 100\,\mu F\,cm^{-2}$). With a developed film, the low frequency capacity values cannot only be explained by a reduction of the active electrode surface area and one explanation could be that the

Table 1. Calculated values from anodic electrochemical impedance diagram of carbon steel (XC38) electrode in 3% NaCl + 5×10^{-2} M $C_{10}H_{21}PO_4Na_2$

i_a ($\mu A\,cm^{-2}$)	R_{HF} ($\Omega\,cm^2$)	$F_{C_{HF}}$ (Hz)	C_{HF} ($\mu F\,cm^{-2}$)	R_{BF} ($\Omega\,cm^2$)	$F_{C_{BF}}$ (Hz)	C_{BF} ($\mu F\,cm^{-2}$)
50	12	10 000	1.3	3200	0.06	830
120	35	6300	0.8	1700	1.20	78
200	60	6000	0.4	1150	8.5	16

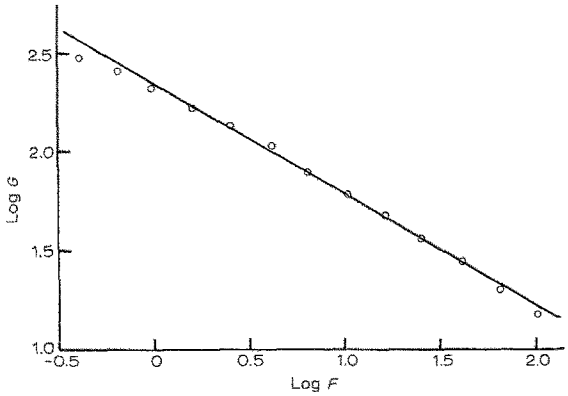

Fig. 3. Log G against log F, for the HF range of Fig. 2.

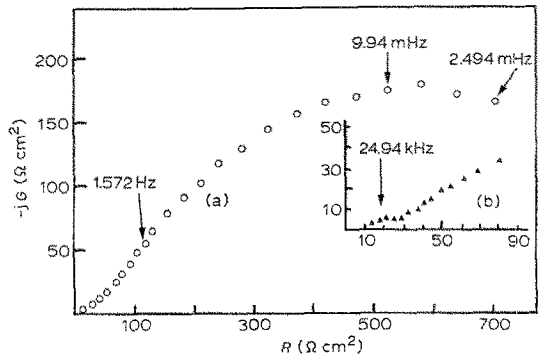

Fig. 4. Electrochemical galvanostatic impedance diagram in the presence of 5×10^{-2} M $C_{10}H_{21}PO_4Na_2$. The electrode was maintained for 2 h at E_{corr} before the measurements. The insert represents the HF range on expanded scale.

pores are collapsing as the film dissolves under these conditions.

With $i_a > 500\,\mu A\,cm^{-2}$ only one capacitative loop is observed. It is important to note that it was difficult at this current density to carry out precise low frequency impedance measurements. Estimated values of the resistance, R, of the characteristic frequency, F_c, and of the associated capacity of the observed loop C are reported in Table 2. In this case the value of the capacity C is still very low. This indicates the presence of a superficial film which is more continuous and more compact than in the preceding case.

The origin of this film may be a transformation of a first film which was initially porous, due to an acceleration of the dissolution process. From this observation the process of blocking starting at low overvoltages on the uncovered surface is confirmed.

The observed capacitative loop is the result of both the influence of the film as well as the charge transfer. The strong hydrophobicity of the studied compound would be consistent with the very low observed capacity value compared to the capacity values in the case of less polar solvents (reduction of the dielectric constant in the double layer).

3.2. *Carbon steel (XC38) – 3% NaCl + 3 × 10⁻³ M C_6H_7NS*

We reported in Fig. 5 the potentiostatic cathodic response of a carbon steel (XC38) electrode in contact with 3% NaCl and with 3% NaCl + 3×10^{-3} M C_6H_7NS. It is clear that the presence of C_6H_7NS considerably decreases the cathodic current. The plateau limiting current is lower than the blank diffusion current. In order to attribute the decrease of diffusion current to the action of C_6H_7NS at the interface (XC38)–3% NaCl, we worked in the same conditions but with a platinum working electrode. In this case, a less marked decrease in the diffusion current was noticed. The absence of corrosion products in the case of the platinum electrode suggests that the decrease in i_L is due to the adsorption of C_6H_7NS. This adsorption can also be produced on the steel (XC38) to form a strongly adsorbed inhibition film. This is confirmed visually by the absence of corrosion products on the carbon steel surface in contact with 3% NaCl + 3×10^{-3} M C_6H_7NS [12, 13].

The form of the curve in the immediate vicinity of E_{corr} reflects a diffusion-controlled cathodic reaction over a restricted overvoltage range. In this case the corrosion current density is identical to i_L and equal to $30\,\mu A\,cm^{-2}$. A large linear region appears in a semi-logarithmic representation. The extrapolation of the straight line obtained to E_{corr} gives the same value as i_{corr}. This linearity may be attributed to the reduction reaction of water displaced towards positive potentials when C_6H_7NS is present. The same phenomenon has been reported elsewhere and attributed to a decrease of interfacial pH [12] although the pH of the bulk solution was not modified.

In the anodic range, the galvanostatic curves show an increase of the overvoltage in the neighbourhood

Table 2. Parameters derived from electrochemical impedance measurements for the carbon steel (XC38) electrode in 3% NaCl + 5 × 10^{-2} M $C_{10}H_{21}PO_4Na_2$

i_a ($\mu A\,cm^{-2}$)	R ($\Omega\,cm^2$)	F_c (Hz)	C ($\mu F\,cm^{-2}$)
500	950	150	1.1
1000	650	630	0.3

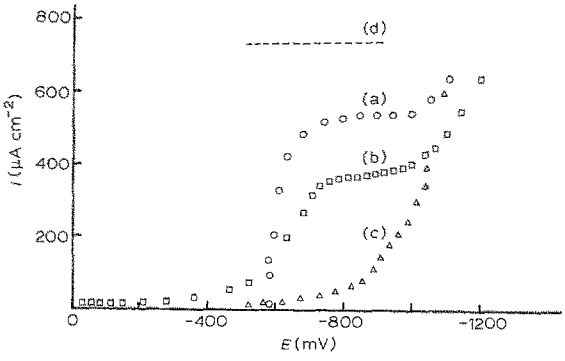

Fig. 5. Current–voltage characteristics with cathodic potentiostatic polarization. The electrode was maintained for 30 min at E_{corr} before measurements, N = 1000 r.p.m. (a) Carbon steel (XC38) – 3% NaCl interface, (b) Pt–3% NaCl + 3×10^{-3} M OATP interface, (c) (XC38) – 3% NaCl + 3×10^{-3} M OATP, (d) diffusion current obtained with a platinum working electrode in contact with 3% NaCl which is noticed to be equal to the current calculated according to the equation of Levich.

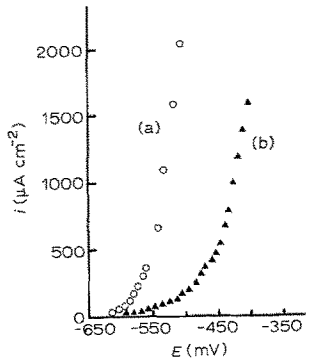

Fig. 6. Steady-state current–voltage characteristics for (a) XC38–3% NaCl; (b) XC38–3% NaCl + 3 × 10^{-3} M C_6H_7NS. N = 1000 r.p.m.

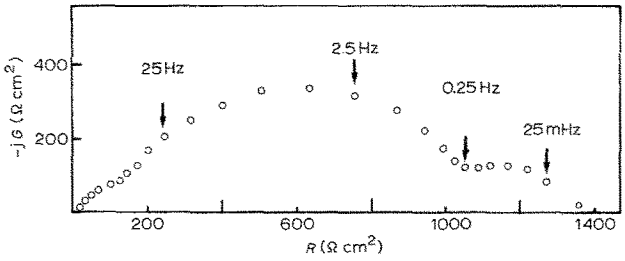

Fig. 7. Electrochemical potentiostatic impedance diagram at E_{corr} for carbon steel (XC38)–3% NaCl + 3 × 10^{-3} M C_6H_7NS interface. N = 1000 r.p.m.

of E_{corr} (see Fig. 6). However, for high overvoltages, the inhibitor does not influence the electrode behaviour. The slope of the anodic Tafel line is 100 ± 10 mV decade^{-1}. Extrapolation to E_{corr} yields a corrosion rate of 25 μA cm^{-2}.

Figure 7 illustrates the electrochemical impedance in the complex plane obtained for a rotating electrode ($\omega = 2\pi N$, where N is the number of electrode revolutions per unit time) having been maintained for 2 h at E_{corr} before starting the measurements. Three capacitative loops are observed. Values of the resistance R_{HF} and of the capacity C_{HF} associated to the HF loop are given in Table 3.

The change in size of the high frequency loop around the corrosion potential is insignificant. It should be noted that the angular electrode speed does not influence the results. When the concentration of C_6H_7NS is decreased, the size of the loop is considerably reduced and vanishes when the concentration of C_6H_7NS is less than 10^{-3} M. High frequency loops have been reported in the literature [13–15].

Simultation techniques have shown that the high frequency loop can be attributed to the formation of a thick, compact inhibiting film [15, 16].

In the anodic range, the size of the intermediate frequency (MF) loop is reduced with increasing overvoltage. It is important to note that for 50 μA cm^{-2} $\leqslant i_a \leqslant$ 1000 μA cm^{-2}, the product $R_{MF}\ i_\alpha$ is constant (see Table 4). The slope of the corresponding Tafel line ($2.3R_{MF}i_\alpha$) is 83 mV. When the experimental errors are considered, this value is close to the value obtained for the blank (74 mV) [17]. Thus the orthoaminothiophenol (C_6H_7NS) acts as a corrosion inhibitor without changing the mechanism of the anodic process. The high corrosion inhibition efficiency is the result of a simple decrease in the active area of the working electrode.

In the anodic range, the low frequency loop decreases in size in phase with the reduction of the high frequency loop. The low frequency loop vanishes at high overvoltages. No interpretation of the evolution of the low frequency loop is offered here.

4. Discussion

From the study of inhibition effect of four organic compounds, three of which are surfactants, on the corrosion of carbon steel (XC38)–3% NaCl interfaces carried out here and in the previous paper [9], we observe that:

(i) The corrosion inhibition of carbon steel (XC38) in 3% NaCl seems to be independent of the species polar head of the organic compounds used. However, electrochemical measurements indicate that there is a difference in the mechanism of inhibition.

In the case of dodecyl sodium phosphonate the corrosion inhibition is the result of a mixed action on both the cathodic and anodic processes. The fact that the limiting current plateau of oxygen reduction was not properly formed, may be attributed to the establishment of a surface film which reduces the pH at the interface. The potential onset of water reduction is therefore displaced and then influences the appearance of the plateau of the limiting reduction current. This film is probably not thick since, in all cases, the impedance measurements did not show a capacitative loop at high frequencies. We suggest that the inhibitor is adsorbed by its anionic polar head. The appearance of a Warburg impedance at E_{corr} over a large range of high frequencies favours the hypothesis of a mixed electrochemical process controlled by both activation and diffusion mechanisms.

In the presence of n-undecylimidazole, the effect is properly observed at cathodic potentials for low concentrations (reduction of i_L) but at high concentrations is observed anodically. The slopes of the Tafel lines and inhibition efficiencies show that this compound acts through a modification of electrochemical

Table 3. Values of high frequency resistance and capacity at different current densities for carbon steel (XC38) in 3% NaCl + 2 × 10^{-3} M C_6H_7NS; temperature 20° C, N = 1000 r.p.m.

i ($\mu A\ cm^{-2}$)	−300	−200	−60	−20	0	+20	+40	+80	+200	+400
R_{HF} (Ω cm^2)	24 ± 2	100 ± 20	85 ± 10	90 ± 10	100 ± 10	90 ± 13	100 ± 10	80 ± 10	32 ± 2	5 ± 2
C_{HF} (μF cm^{-2})	–	2.3 ± 0.4	4.5 ± 0.5	5.8 ± 1	3.5 ± 0.8	4.6 ± 0.3	4.0 ± 0.2	5 ± 1	3.8 ± 0.4	3.2 ± 0.2

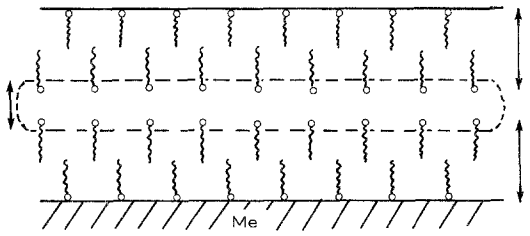

Fig. 8. Double layer piling (stacking) structure of surfactant compound adsorption at metal–3% NaCl interface.

processes at the interface. In this case the high frequency capacitative loop was not detected with certainty and we again propose that adsorption occurs through the polar head of the inhibitor. The hydrophobic character of the hydrocarbon chain favours the stability of a third film on top of the adsorbed film and, as a result, a bilayer structure is established (see Fig. 8). The bilayer hypothesis is consistent with the inhibition characteristics observed for this organic compound and must be consistent with a stable thin film.

A series of bilayers of this type may be envisaged on the electrode so long as the local concentration is below the critical micellar concentration, C.M.C., (see [9]). However, the number of such layers will depend, not only on the concentration and the surfactant type, but also on the dynamics of thermal stability of such layers (Brownian notion/convection).

(ii) In the case of orthoaminothiophenol (OATP), the entire electrochemical data can be explained in terms of a film effect generated by C_6H_7NS at the electrode surface. The impedance diagram resembles published results for similar electrodes covered with a paint film [16]. The mechanism of inhibition was found to be essentially physical, i.e. a reduction of active surface area by the inhibitor with no change in the corrosion mechanism [18]. Our electrochemical data are consistent with such a model since it has shown that the kinetics of the anodic and cathodic processes are not modified by the inhibitor (values of b_a and b_c remain constant). The high frequency loop of the impedance diagram reported in Fig. 7 can be ascribed to a relatively compact and thick inhibitor film, whereas the remaining part of the diagram represents the faradaic process on the free film sites. This agrees well with previously published results [19]. The protective characteristics of the inhibitor film can be characterized by the values of C_{HF} and R_{HF} determined from electrochemical impedance measurements carried out at the corrosion potential E_{corr}.

Finally, the development of a relatively compact and thick protective film of C_6H_7NS on the metal surface can be explained by considering the molecular structure of this compound: (a) the presence of two heteroatoms (N and S) and the aromatic cycle for aqueous systems always gives a strong adsorption bonding for the molecules, i.e., good adherence and compactness of the film; (b) the possible occurrence of a stacking phenomenon between the molecules may also lead to an increase in film thickness.

The same adsorption mechanism seems applicable in the case of dodecyl sodium phosphate ($C_{10}H_{21}PO_4Na_2$). The thick film inferred in this case would be stabilized by corrosion products. In fact the high frequency loop was only observed when the electrode is maintained in the electrolyte at the corrosion potential for long periods before measurement or otherwise pretreated in the anodic domain. This may be explained by a preferential adsorption of the surfactant onto the cathodic sites.

(iii) The difference in the mechanism of corrosion inhibition of carbon steel in NaCl (3%) in the presence of dodecyl sodium phosphonate compared to dodecyl sodium phosphate can be justified by the difference of the polar head.

The ether type oxygen of phosphates RPO_4^{2-} linked to the alkyl electron donor group behaves in a different manner to the other three oxygens which are

Table 4. Variation of parameters evaluated in the intermediate frequency range (MF) as a function of applied current densities for the interface carbon steel (XC38) – 3% NaCl + 3 × 10^{-3} M OATP: N = 1000 r.p.m., electrode maintained for 1 h in the electrolyte at E_{corr} before measurements

i ($\mu A\,cm^{-2}$)	R_{MF} ($\mu\,cm^2$)	$F_{C_{MF}}$ (Hz)	C_{MF} ($\mu F\,cm^{-2}$)	iR_{MF} (mV)
−400	980 ± 25	0,160 ± 0,006	1015 ± 300	392 ± 10
−300	1400 ± 60	0,063 ± 0,005	1805 ± 200	420 ± 10
−150	1700 ± 70	0,063 ± 0,004	1490 ± 200	255 ± 10
−90	1900 ± 50	0,07 ± 0,01	1200 ± 180	171 ± 4,5
−70	2300 ± 60	0,10 ± 0,01	700 ± 85	161 ± 5
−50	2000 ± 100	0,20 ± 0,01	400 ± 40	100 ± 5
−30	1500 ± 80	0,60 ± 0,02	200 ± 40	45 ± 3
0	940 ± 20	4,0 ± 0,1	42 ± 2	-
+20	800 ± 15	10,0 ± 0,1	20 ± 2	16 ± 1
+50	680 ± 10	9,50 ± 0,05	27 ± 3	34 ± 1
+80	400 ± 8	6,1 ± 0,1	84 ± 20	32 ± 2
+200	170 ± 10	12,5 ± 0,5	80 ± 12	34 ± 2
+300	120 ± 6	14 ± 1	120 ± 36	36 ± 2
+500	78 ± 6	16 ± 1	124 ± 11	39 ± 3
+1000	34 ± 2	30 ± 2	156 ± 18	34 ± 2
+3000	20 ± 3	40 ± 2	199 ± 35	60 ± 9

either directly or indirectly of identical electronic characteristics by the mesomeric process according to:

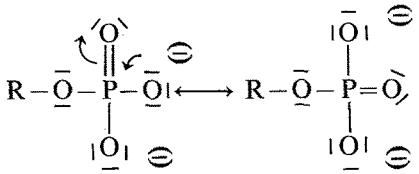

A "soft" characteristic is attributed to the oxygen of the ether type while other phosphate oxygens have "hard" characteristics [20].

In the case of RPO_3^{2-} phosphonates, analogous reasoning allows attribution of the hard character to all the oxygens. Iron, as a transition metal is considered in its atomic state to be a "soft" element while the cation Fe^{2+} is "harder" [21].

In the phosphate case, the oxygen type ether, considered as a "soft" base, associate with atomic iron considered as a "hard" acid while the other oxygens, "soft bases", associate with ferrous ions Fe^{2+} considered as "harder" acid [20]. A non negligible "symbiotic" effect is probably associated with the formed complex [22].

The mesomeric considerations applied to the phosphates RPO_4^{2-} results in a limiting case where the ether–type oxygen carries a partial positive charge. This limiting form is active on the cathodic iron sites.

Acknowledgement

The authors are indebted to Dr Max Costa "Directeur du Laboratoire d'Electrochimie Interfaciale du CNRS" and to Dr Robert Reeves for stimulating and fruitful discussion and comment. The technical help of Mrs Yvette Rodier and Mr Charles Mathieu is also gratefully acknowledged.

References

[1] G. W. Walter, *Corros. Sci.* **15** (1975) 47; *ibid.* **16** (1976) 573.
[2] K. G. Boto and L. F. G. Williams, *J. Electrochem. Soc.* **124** (1977) 656; *J. Electroanal. Chem* **77** (1977) 1.
[3] D. D. McDonald, B. C. Syrett and S. S. Wing, *Corrosion* **34** (1978) 289, *ibid.* **35** (1979) 367.
[4] A. Bonnel, F. Dabosi, C. Deslouis, M. Duprat, M. Keddam and B. Tribollet, *J. Electrochem. Soc.* **130** (1983) 753; F. Dabosi, C. Deslouis, M. Duprat and M. Keddam, *J. Electrochem. Soc.* **130** (1983) 761. 'd'Electrochimie', Dubrovnik, 13–18 September 1981.
[5] J.O'M. Bockris and P. K. Subramanyan, *Corr. Sci.* **10** (1970) 435.
[6] Z. Takehara, A. Saito and S. Yoshizawa, *ibid* **16** (1976) 91.
[7] A. A. Abdul Azim and S. H. Sanad, *ibid.* **12** (1972) 337.
[8] T. Shibata, G. Okamoto, A. Murao and T. Tsuchida, *Trans. Iron and Steel Inst., Japan* **9** (1969) 239.
[9] F. Dabosi, Y. Derbali, M. Etman, A. Lattes, A. de Savignac and A. Srhiri, *J. Appl. Electrochem.* **21** (1991) 255–260.
[10] M. Duprat, F. Moran and F. Dabosi, *Corr. Sci.* **23** (1983) 1047.
[11] F. M. Stern and A. L. Geary, *J. Electrochem. Soc.* **104** (1957) 56.
[12] F. El Taib Heakal and S. Haruyama, *Corr. Sci.* **20** (1980) 887.
[13] A. Srhiri, H. Duprat, T. Picaud, A. Ben-Bachir and F. Dabosi, *J. Chim. Phys.* (1989), submitted.
[14] A. Bonnel, F. Dabosi, C. Deslouis, M. Duprat, M. Keddam and B. Tribollet, '160e Colloque de l'Electrochemical Society', Denver (11–16 October 1981).
[15] F. Moran, 'Thèse de 3e Cycle', Toulouse, France (1984).
[16] A. Bonnel, M. Duprat, F. Dabosi, J. Durand and L. Cot, *J. Appl. Electrochem.* **12** (1982) 711.
[17] M. Duprat, 'Thèse d'Etat', Toulouse, France (1981).
[18] L. Beaunier, I. Epelboin, J. C. Lestrade and H. Takenouti, *Surf. Technol.* **4** (1976) 237.
[19] F. Dabosi, C. Deslouis, M. Duprat and H. Takenouti, Proc. Int. Symp. 'Fundamental Aspect of Corrosion Protection by Surface Modification' (edited by E. MacCaferty, C. R. Clayton and J. Oudar), Electrochemical Society Meeting, Washington (October 1983) p. 260.
[20] J. Seyden Penne, *Bull. Soc. Chim., France* **9** (1968) 3871.
[21] R. G. Pearson, *Chem. Brit.* **3** (1967) 103.
[22] R. G. Pearson and J. Songstad, *J. Amer. Chem. Soc.* **89** (1967) 1827.